

This article was downloaded by: [University of Illinois at Urbana-Champaign]

On: 30 January 2015, At: 19:56

Publisher: Taylor & Francis

Informa Ltd Registered in England and Wales Registered Number: 1072954 Registered office: Mortimer House, 37-41 Mortimer Street, London W1T 3JH, UK



## Philosophical Magazine A

Publication details, including instructions for authors and subscription information:

<http://www.tandfonline.com/loi/tpha20>

### A model for the anelastic straining of saline ice subjected to cyclic loading

David M. Cole <sup>a</sup>

<sup>a</sup> US Army Cold Regions Research and Engineering Laboratory ,  
Hanover, New Hampshire, USA

Published online: 27 Sep 2006.

To cite this article: David M. Cole (1995) A model for the anelastic straining of saline ice subjected to cyclic loading, *Philosophical Magazine A*, 72:1, 231-248, DOI: [10.1080/01418619508239592](https://doi.org/10.1080/01418619508239592)

To link to this article: <http://dx.doi.org/10.1080/01418619508239592>

PLEASE SCROLL DOWN FOR ARTICLE

Taylor & Francis makes every effort to ensure the accuracy of all the information (the "Content") contained in the publications on our platform. However, Taylor & Francis, our agents, and our licensors make no representations or warranties whatsoever as to the accuracy, completeness, or suitability for any purpose of the Content. Any opinions and views expressed in this publication are the opinions and views of the authors, and are not the views of or endorsed by Taylor & Francis. The accuracy of the Content should not be relied upon and should be independently verified with primary sources of information. Taylor and Francis shall not be liable for any losses, actions, claims, proceedings, demands, costs, expenses, damages, and other liabilities whatsoever or howsoever caused arising directly or indirectly in connection with, in relation to or arising out of the use of the Content.

This article may be used for research, teaching, and private study purposes. Any substantial or systematic reproduction, redistribution, reselling, loan, sub-licensing, systematic supply, or distribution in any form to anyone is expressly forbidden. Terms & Conditions of access and use can be found at <http://www.tandfonline.com/page/terms-and-conditions>

## A model for the anelastic straining of saline ice subjected to cyclic loading

By DAVID M. COLE

US Army Cold Regions Research and Engineering Laboratory,  
Hanover, New Hampshire, USA

[Received 18 April 1994† and accepted 23 December 1994]

### ABSTRACT

This work formulates a model of the anelastic response of saline ice based on dislocation and grain-boundary relaxations. The dislocation-based mechanism generally dominates the behaviour, having a relaxation strength of approximately an order of magnitude greater than the grain-boundary relaxation. The latter process explains the anelasticity observed at higher frequencies and lower temperatures.

An expression for the oscillatory motion of basal plane dislocations is developed that derives its temperature dependence from the dislocation drag term, which is found to be approximately the same as in freshwater ice. The results of a frequency shift analysis indicate that the dislocation relaxation may be described by a single activation energy and a distribution in relaxation time. The model applies to the region of behaviour that is approximately linear in stress.

Predictions of transient and steady-state cyclic loading behaviour are examined in detail and compared with experimental observations. Aspects of the model that are still under development, related primarily to temperature effects on the microstructure and the incorporation of explicit microstructural parameters, are also discussed.

### § 1. INTRODUCTION

As a consequence of sustained interest in the mechanical properties of sea ice, a number of experimental and theoretical efforts are under way to develop improved models of its behaviour. Since ice in general, and sea ice in particular, exhibits high levels of anelasticity under a wide range of conditions, a complete description of the anelastic component of strain is needed. Although previous work, primarily focused on freshwater ice, indicates that lattice dislocation processes and grain-boundary sliding contribute significantly to ice anelasticity, a useful physically based model incorporating both effects has not therefore emerged. Additionally, since the anelastic strain expression employed in current ice creep models is based on experiments having an evolving microstructure, they are of very limited use in predicting behaviour for constant microstructural conditions.

To gain insight into saline-ice anelasticity under constant microstructural conditions, Cole and Durell (1995) conducted experiments on saline (NaCl) ice employing the reversed direct-stress technique. The experimental observations indicate the operation of a generally dominant dislocation-based relaxation and a grain-boundary mechanism, in keeping with findings for fresh-water ice. The present paper addresses the physical interpretation of those results and the associated model

---

† Received in final form 16 December 1994.

development. The model includes stress, temperature and frequency effects for both mechanisms. Its applicability is restricted to temperatures below  $-10^{\circ}\text{C}$ , although its extension to higher temperatures is currently receiving attention. The model addresses the case of undeformed polycrystals, where the two mechanisms can operate simultaneously, with one or the other dominating, depending on the details of the microstructure, the mobile dislocation density and the experimental conditions.

The experimental results showed a strong influence of total porosity on the dislocation relaxation and quantification of this effect constitutes a major goal of the ongoing effort. However, this aspect of the work is still in progress and the explicit incorporation of microstructural effects is left to the next phase of model development. As a consequence of the relatively low strength of the proton rearrangement mechanism of anelasticity (Onsager and Runnels 1969), and of a high-frequency dislocation resonance peak (Hiki and Tamura 1983), those contributions are ignored here.

## § 2. OVERVIEW OF THE MODEL

Indications in the work of Cole and Durell (1995) of a low-frequency asymptote for the modulus of saline ice for nominally constant microstructural conditions helps to define the strength of the relaxation. It also lends support for a relaxation model as opposed to a high temperature background model.

The analytical expression for the dislocation relaxation comes from consideration of a dislocation oscillating under an applied stress, subjected to lattice drag and a restoring stress composed of an average microstructural stress and line tension. The drag, which is extremely high relative to other materials, is generally believed to be associated with the reorientation of protons that is required for dislocations to move without excessive defect formation (Whitworth 1978, Weertman 1983). At  $-10^{\circ}\text{C}$ , the drag term for basal dislocations in ice is of the order of  $10^2$  Pa s, compared with values typically in the range of  $10^{-5}$ – $10^{-3}$  Pa s for pure metals at temperatures of interest (Mason 1967). However, the drag mechanism is still a matter of speculation and continues to receive attention (Khusnatdinov and Petrenko 1994). The restoring stress term lumps together the effects of dislocation–dislocation interactions, dislocation–obstacle interactions, elastic anisotropy and line tension. A frequency shift analysis indicates that the basal dislocation contribution may be characterized by a single activation energy and a distribution in relaxation time. The model employs a peak-broadening term to address the effect of the relaxation time distribution on the frequency dependence of the anelastic strain. Considerable attention focuses on an adequate description of the initial transient behaviour, since it provides useful insight into the relaxation time characteristics and serves as a link between cyclic and monotonic loading responses.

The following sections examine the experimental findings concerning the characteristics of the two relaxation mechanisms and develop the mathematical expressions for the model in terms of compliance. Subsequently, attention focuses on comparing the model predictions with experimental observations.

## § 3. GRAIN-BOUNDARY ANELASTICITY

Grain-boundary anelasticity in ice has been observed in laboratory-prepared fresh-water ice (Kuroiwa 1965, Tatibouet, Perez and Vassoille 1987, Cole, 1994) and saline ice (Cole and Durell 1995), and in field cores of glacier ice (Nakamura and Abe 1979). The activation energy for the peak appears to be in the range 1.26–1.38 eV, which is considerably higher than the activation energy for self-diffusion (0.7 eV) or

dislocation glide (see below). The kinetics of the relaxation are such that the associated internal friction peak occurs under a 1 Hz forced oscillation between approximately  $-15$  and  $-20^{\circ}\text{C}$ , making it relatively easy to examine with cyclic reversed direct-stress or torsional loading techniques. Although a clear link between grain size and the strength of the relaxation has not been developed, grain size effects have been observed in freshwater columnar ice (Gold 1958, 1994), granular ice (Cole 1994), and field cores of granular glacier ice (Nakamura and Abe 1979). The smallest grain size examined in the latter work (0.7 mm) had an internal-friction peak height of 0.155, but the more common grain sizes in the range 1–10 mm produce peaks in the range 0.06–0.1, which correspond to modulus defects in the range 0.13–0.23. Interestingly, copper exhibits a grain-boundary internal-friction peak of approximately the same strength, activation energy and relaxation time as ice (Shigenaka, Manzen and Mori 1983), and Kê, Cui, Yan and Huang (1984) report peaks of similar magnitude in fine-grain super-high-purity aluminium. Cole and Durell (1995) found the grain-boundary internal-friction peak in saline ice to be independent of the cyclic stress amplitude.

#### § 4. DISLOCATION-BASED ANELASTICITY

As determined in creep recovery experiments on fresh-water polycrystalline ice, the ratio of anelastic to elastic strain ranges from 10 (as obtained by Cole (1991), testing laboratory-grown granular ice in compression at  $-2^{\circ}\text{C} \leq T \leq -10^{\circ}\text{C}$ ) to more than 60 (as obtained by Duval (1978), testing glacier ice in torsional creep at  $T = -1.5^{\circ}\text{C}$ ). These experiments show the build-up of anelastic strain that occurs during primary creep. Observations on fresh-water single crystals oriented for easy glide indicate a smaller ratio (about 6) after a total creep strain of 0.005 (Cole 1992) ( $T = -5^{\circ}\text{C}$ ;  $\sigma_{\text{creep}} = 0.31$  MPa). Apart from the exceptional values obtained by Duval (1978), ice exhibits a relatively high level of creep anelasticity similar to that observed for dislocation-based processes in aluminium (Gibeling and Nix, 1981).

Vassoille, Mai and Perez (1978) linked a rise in the magnitude of internal friction of fresh-water single crystals to increases in the measured dislocation density and modelled the observed internal friction essentially as a high-temperature background. The activation energies from observations of groups of dislocations using X-ray techniques have been in the range 0.55–0.6 eV. Tatibouet *et al.* (1987) demonstrated that creep straining produces a dramatic increase in the dislocation internal friction in addition to causing the grain boundary peak to disappear. Cole (1993) observed the dislocation-based compliance of saline ice to increase markedly with pre-strain. Duval (1978) noted that the time dependence of the recovery process in glacier ice implied a distribution in relaxation times and treated the dislocation internal friction as a high-temperature background. The frequency dependence was addressed in an empirical manner.

Sinha (1978) examined the creep and creep anelasticity (or delayed elasticity, as it is referred to in that work) of columnar fresh-water ice and determined an activation energy of 0.7 eV for both processes. (However, in a review of the literature, Weertman (1983) recommended an activation energy of 0.62 eV for polycrystalline ice creep.) That and subsequent work (Sinha 1990) presented a phenomenological model for ice creep that included an expression for creep anelasticity based on a grain-boundary sliding process.

Vassoille *et al.* (1978) found a somewhat variable apparent activation energy in the range 0.33–0.53 eV from their internal-friction experiments, which is in reasonable agreement with the value of  $0.52 \pm 0.1$  eV found for saline ice (Cole and Durell 1995),

and the value of 0.54 eV for basal slip in single crystals of pure ice under cyclic loading (see Appendix). Observations on groups of basal dislocations in pure ice using X-ray techniques that require long exposure times have produced somewhat higher values of 0.55–0.6 eV (Mai 1976, Fukuda, Hondoh and Higashi 1987). More recently, Shearwood and Whitworth (1991) found activation energies in the range 0.87–0.95 eV for well characterized edge and screw dislocations using synchrotron radiation. Although the experimental technique of the latter workers is superior to that in the earlier studies of dislocation motion, there appears to be no evidence for such high activation energies in mechanical properties experiments involving the motion of large number of dislocations.

From the cyclic loading observations, the dislocation relaxations in both fresh-water and saline ice are large and occur at low frequencies, and both materials exhibit approximately the same activation energy (below the eutectic point). This leads to the view that basal dislocation glide is fundamentally the same in both materials to a first approximation.

Another matter of concern is the potential effect of pinning points of dislocation behaviour. Models of dislocation resonance and relaxation predicated on the bow-out of dislocation segments between pinning points have been widely successful. However, it has been pointed out (Woigard, Riviere and De Fougnet 1981) that such models frequently cannot simultaneously explain both the magnitude and the relaxation time of high-temperature processes. Bow-out models require the presence of pinning points (from point defects and dislocation interactions) but X-ray topographs in fresh-water ice consistently show that basal dislocation segments and semihexagonal loops expand freely (Liu, Baker, Yao and Dudley 1992). Hiki and Tamura (1983) found that a bow-out model with a loop length of  $10^{-6}$  m adequately explained their observations of a dislocation resonance peak in the megahertz range in ice containing a 0.33 at. p.p.m. concentration of  $\text{Na}^+$  acting as pinning points. If pinning points with this concentration were effective in the low-frequency process in saline ice, and considering line tension as the restoring force (Lenz and Lücke 1975), the relaxation peak would occur near 2 Hz (for  $-10^\circ\text{C}$  and using a suitably high value of 40 Pa s for the drag term). However, the experimental results show no relaxation peak for those conditions. Rather, one occurs at significantly lower frequencies (between  $10^{-4}$  and  $10^{-3}$  Hz), which cannot be explained by that model. Thus, since there is no evidence of pinning point effects when large dislocation excursions are involved, the present model does not employ a segment length term.

## § 5. MODEL DEVELOPMENT

### 5.1. *Dislocation relaxation*

#### 5.1.1. *Oscillatory motion of dislocations*

The physical basis for this relaxation is the oscillatory motion of basal plane dislocations under a sinusoidally varying stress. The assumptions of the model and their consequences are as follows.

- (1) On the bases of the observation of a low-frequency asymptote in the modulus of saline ice, the dislocation-based anelasticity is formulated as a relaxation process rather than high-temperature background.
- (2) Since virtually no change in cyclic loading behaviour results from continuous load cycling at stress levels very close to the tensile strength, the dislocation density is taken to remain constant for the prevailing conditions.

- (3) Given the observations that saline ice obeys time–temperature superposition to a good approximation and that the peak is relatively broad, the underlying relaxation process is characterized by a unique activation energy and a distribution of relaxation times.
- (4) The dislocation velocities are sufficiently low to ignore inertial effects. Their motion under forced oscillation can thus be described by a temperature-dependent drag term and an opposing force term related to line tension and microstructural stress.

The model accounts for temperature effects on the anelastic straining only and not as yet for temperature effects on either the elastic modulus or the porosity. Additionally, the model applies to material having a microstructure that has metamorphosed into discrete brine- or gas-filled inclusions in a pure ice matrix and does not apply to newly formed sea ice, which may exhibit significantly different temperature effects. The quantities in this section pertain to the dislocation relaxation only. Superscripts are introduced in a subsequent section when it is necessary to discriminate between the two relaxation processes.

The governing equation for the oscillatory motion of dislocations under a slowly varying stress field is taken as

$$B\dot{x} + Kx = b\sigma \sin(\omega t), \quad (1)$$

where  $x$  is the distance,  $B$  is the temperature-dependent dislocation drag,  $K$  is the restoring stress acting in opposition to the dislocation,  $b$  is the Burgers vector,  $\sigma_0$  is the maximum cyclic shear stress resolved on the slip plane,  $\omega$  is the angular frequency and  $t$  is the time. Weertman (1955) presented a relationship similar to eqn. (1) and discussed the significance of  $K$  and its evaluation in the context of an internal-friction model applicable at higher frequencies than the present study. Kressel and Brown (1967) and Joncich (1976) employed relationships similar to eqn. (1) in analyses of microstrain experiments of nickel and creep anelasticity in ice respectively. Lenz and Lücke (1975) reviewed similar modelling approaches in the context of dislocation resonance damping, which has many elements in common with the present effort. They pointed out that experimental measurements allow determination of the ratios of various model parameters:  $\Delta/K$ ,  $B/K$  and  $B/\Delta$ , where  $\Delta$  is the mobile dislocation density. More recently, Lakki, Schaller, Nauer and Larry (1993) applied a similar approach to model the internal friction of yttria-doped zirconia polycrystals. As in the present work, they also employed a peak-broadening term and note that the predicted internal friction reduces to an exponentially increasing function of temperature as the restoring stress  $K$  becomes small.

The solution to eqn. (1) has the form

$$x = \left[ C_0 + \frac{b\sigma_0}{B} \int \sin(\omega t) \exp\left(\int \frac{K}{B} dt\right) dt \right] \exp\left(-\int \frac{K}{B} dt\right). \quad (2)$$

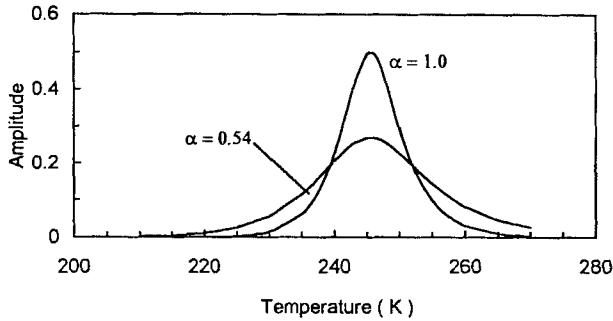
The solution to eqn. (2) is

$$x = C_0 \exp\left(-\frac{Kt}{B}\right) + \frac{b\sigma}{B} \frac{(K/B) \sin(\omega t) - \omega \cos(\omega t)}{(K/B)^2 + \omega^2}. \quad (3)$$

Application of the initial conditions of  $x = 0$  at  $t = 0$  yields the value of

$$C_0 = \frac{b\sigma}{B} \frac{\omega}{(K/B)^2 + \omega^2}. \quad (4)$$

Fig. 1



The curve labelled  $\alpha = 1.0$  gives the value of the bracketed term in eqn. (7) against temperature.

The first term in eqn. (3) determines the transient behaviour and the second is the steady-state response. After grouping terms, the coefficient of the cosine function in eqn. (3) describes a relaxation peak with a central frequency determined by the value of  $K/B$ . The temperature dependence of the peak stems from the temperature dependence of the drag term  $B$ :

$$B = B(T) = B_0 \exp\left(\frac{Q}{kT}\right). \quad (5)$$

This expression for dislocation drag pertains to basal slip in pure ice and is expected to be independent of the microstructure.  $B_0$  and  $Q$  in eqn. (5) are evaluated in the Appendix.

A relaxation time  $\tau = B/K$  may be associated with the peak, which upon substitution into eqns. (3) and (4) yields

$$x = C_0 \exp\left(-\frac{t}{\tau}\right) + \frac{b\sigma \sin(\omega t) - \tau\omega \cos(\omega t)}{K \sqrt{1 + (\tau\omega)^2}}, \quad (6)$$

$$C_0 = \frac{b\sigma}{K} \frac{\tau\omega}{\sqrt{1 + (\tau\omega)^2}}. \quad (7)$$

The sine and cosine terms determine the components of the dislocation strain that are in phase and  $90^\circ$  out of phase respectively with the applied stress. The curve labelled  $\alpha = 1.0$  in fig. 1 is the amplitude of the bracketed term in eqn. (7), which governs the frequency response of the model. The parameter  $\alpha$  determines the peak width as discussed in a subsequent section.

Given that the temperature-dependent drag term is known from independent observations,  $K$  can be assessed from the central frequency of the relaxation peak as indicated in the compliance and modulus data shown in fig. 10 and 14 of the paper by Cole and Durell (1995).

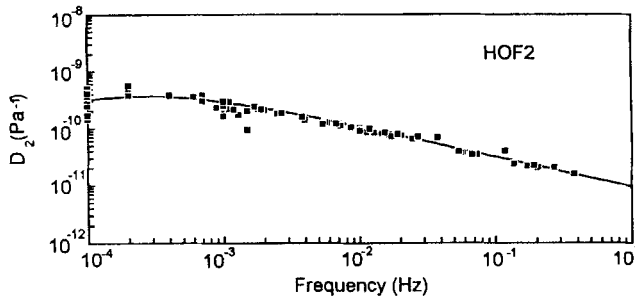
### 5.1.2. Relaxation time distribution

The distribution in  $\tau$  results from the net contributions from a great number of discrete systems distributed throughout the specimen, each with its own characteristic geometry, and hence relaxation time. The effect of the distribution in  $\tau$  may be addressed analytically either by substituting an alternative frequency function in eqn. (6) or by

Model parameters for dislocation relaxation optimized for each specimen.

Specimen	$\delta D^d$ (Pa <sup>-1</sup> )	$\alpha^d$	$K$ (Pa)
HOF1	$1.4 \times 10^{-9}$	0.53	0.07
HOF2	$1.4 \times 10^{-9}$	0.53	0.07
HOP2	$1.4 \times 10^{-9}$	0.55	0.05
PL19	$1.8 \times 10^{-9}$	0.59	0.07

Fig. 2



The log-plot of compliance against frequency for the results from specimen HOF2 (Cole and Durell 1995). The points have been shifted to lie along a  $T = -10^\circ\text{C}$  master curve. The line is the model prediction with parameter values as indicated in the text.

incorporating an estimate of the relaxation time distribution  $l(\ln \tau)$  and employing the expression (Ferry 1981)

$$D_2(\omega) = \int_{-\infty}^{+\infty} l(\ln \tau) \frac{\tau \omega}{1 + (\tau \omega)^2} d(\ln \tau). \quad (8)$$

Ferry (1981) presented a method for approximating the relaxation time distribution if the compliance is known over a sufficiently wide frequency range. It is noted in passing that calculations carried out using eqn. (8) with  $l(\ln \tau)$  estimated using Ferry's method agreed well with the experimental observations. However, the calculations can be simplified with no loss in accuracy by employing an alternative frequency dependence of the form

$$\frac{\alpha}{2} \operatorname{sech}(\alpha s), \quad (9)$$

where  $s = \ln \tau \omega$ . Equation (9) reduces to the Debye expression for  $\alpha = 1$  and has been used in place of the Debye term  $\tau \omega / [1 + (\tau \omega)^2]$  in similar applications for crystalline materials (Nowick and Berry 1972). Figure 1 shows the relaxation peaks associated with  $\alpha = 0.54$  together with the Debye peak ( $\alpha = 1.0$ ). The distribution broadens as  $\alpha$  decreases, but its integral value remains unchanged. A least-squares error analysis of the frequency-shifted data given by Cole and Durell (1995) produced estimates of  $\alpha$ ,  $\delta D$  and  $K$  for several specimens (see the table). Figure 2 illustrates the frequency-shifted data points for a typical specimen from Cole and Durell (1995). The solid line is the model prediction, as discussed in the next section, based upon the parameter values given in the table.

### 5.1.3. Dynamic compliance

Employing eqns. (9) and (6) results in the loss compliance  $D_2^d$  of

$$D_2^d = \alpha^d \delta D^d \frac{1}{\exp(\alpha^d s) + \exp(-\alpha^d s)}. \quad (10)$$

The storage compliance  $D_1^d(\omega)$  is

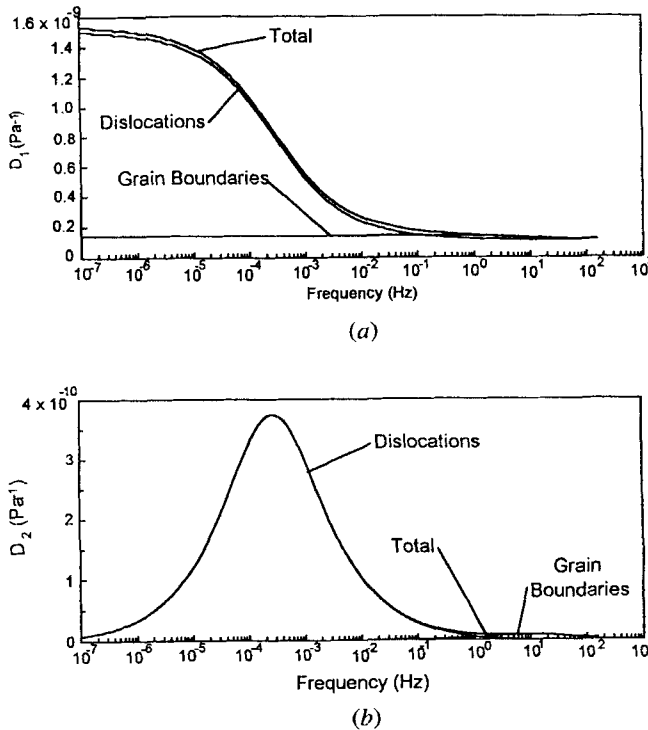
$$D_1^d(\omega) = D_u^d + \frac{2}{\pi} \int_{s_i}^{+\infty} D_2^d d[\ln(\tau\omega)], \quad (11)$$

where the lower limit of integration  $s_i$  corresponds to the value of  $\ln(\tau\omega)$  of interest. Upon integration, eqn. (11) yields

$$D_1^d(\omega) = D_u^d + \delta D^d \left( 1 - \frac{2}{\pi} \tan^{-1} [\exp(\alpha^d s_i)] \right). \quad (12)$$

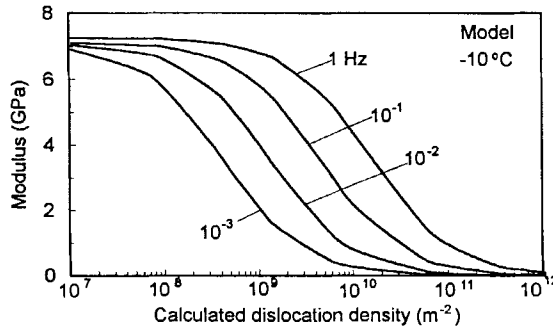
Figure 3 shows the dynamic compliances as a function of frequency for the relaxation, computed for  $T = -10^\circ\text{C}$ . Equations (10) and (12) define the dislocation relaxation and these, together with analogous expressions for the grain-boundary relaxation (discussed in the next section), fully define the model.

Fig. 3



Model predictions of the dynamic compliances as a function of frequency for the dislocation and grain-boundary relaxations, calculated for  $-10^\circ\text{C}$ : (a) the storage compliance  $D_1$ ; (b) the loss compliance  $D_2$ .

Fig. 4



Model predictions of modulus against mobile dislocation density for frequencies as indicated.

#### 5.1.4. Relationship between dislocation density and compliance

The dislocation contribution to the total strain  $\varepsilon_d$  is

$$\varepsilon_d = \Delta \Omega b x_d, \quad (13)$$

where  $\Delta$  is the dislocation density,  $\Omega$  is an orientation factor,  $b$  is the Burgers vector and  $x_d$  is given by eqn. (6). Examination of eqns. (10) and (13) indicates that

$$\delta D^d = \frac{\Delta \Omega b^2}{K}. \quad (14)$$

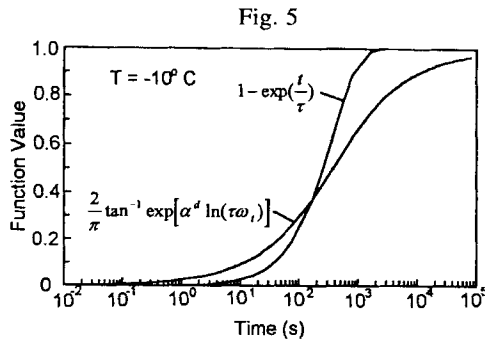
The specimen compliance change ascribable to dislocations is thus a linear function of the mobile dissociation density  $\Delta$  and inversely proportional to  $K$ . The orientation factor  $\Omega$  is estimated as  $\pi^{-1}$  for the S2 columnar ice under consideration;  $K$  was estimated from the experimental results to be approximately 0.07 Pa as discussed in an earlier section, and  $b = 4.52 \times 10^{-10}$  m. The estimated value of  $\delta D = 1.4 \times 10^{-9} \text{ Pa}^{-1}$  leads to a reasonable value for the mobile dislocation density of  $1.5 \times 10^9 \text{ m}^{-2}$ . Figure 4 shows the predicted initial modulus as a function of the mobile dislocation density on the basal planes for four frequencies. It has not yet been possible to verify the predicted values directly, however, because the dislocation density has proven to be too high to allow discrimination of individual dislocations in topographs employing synchrotron radiation (I. Baker 1994, private communication).

#### 5.1.5. Transient behaviour

The transient behaviour is governed by the term  $\exp(-t/\tau)$  in eqn. (6). The experiments indicated that the duration of the transient effects scaled with the driving frequency, that they persisted past the end of the first cycle and that the hysteresis loops are not centred about the point ( $\varepsilon = 0, \sigma = 0$ ), but exhibit a bias in the direction of initial loading. Using a constant relaxation time  $\tau = 1/\omega_0$  (where  $\omega_0$  is the central frequency of the dislocation relaxation peak) produces transient effects that proceed too slowly for driving frequencies greater than  $\omega_0$ . The expression

$$\frac{2}{\pi} \tan^{-1} \{ \exp[\alpha^d \ln(\tau \omega_i)] \}, \quad (15)$$

where  $\tau = 1/\omega$  ( $\omega$  is the angular driving frequency), however, which uses the frequency dependence of  $D_1^d$  (see eqn. (12)), adequately describes the observed transient behaviour. Time enters the expression explicitly by setting  $\omega_i = t^{-1}$  (Ferry 1981).



Function values against time for a simple exponential and the transient function employed in the analysis.

Figure 5 shows a plot of  $[1 - \exp(-t/\tau)]$  against time for  $\tau = 1/\omega$  together with the transient function described in the preceding paragraph. The peak-broadening effect of the relaxation time distribution prolongs the transient effects, thereby producing hysteresis loops that are offset appropriately from the origin. Although it is assumed that the form of the relaxation time distribution is not a function of the applied frequency, it is recognized that this may not be the case.

The anelastic strain effectively vanished for 1 Hz and  $-30^\circ\text{C}$  for the stress levels under consideration. This corresponds to  $D_1^d \approx 1.2 \times 10^{-10} \text{ Pa}^{-1}$ , or to a threshold value of 0.065 of the transient function (which runs from zero to unity). The model employs this threshold value, and the transient function value is scaled appropriately to maintain its range from zero to unity.

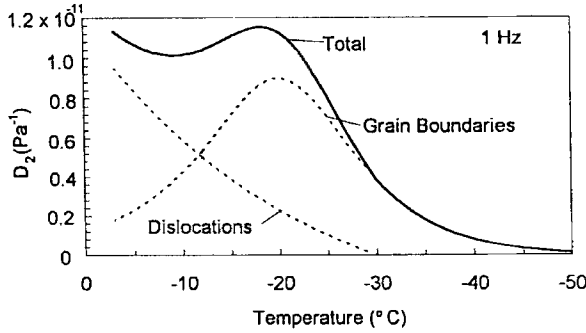
The physical interpretation of the foregoing analysis is that elements with progressively longer relaxation times are able to operate fully as the driving frequency decreases, and the time required for the transient to subside consequently increases as well. Based on physical reasoning, the relaxation times are distributed about  $\tau_m$  when the driving frequency drops below  $1/\tau_m$ .

### 5.2. Grain-boundary relaxation

The saline-ice data do not allow for a reliable estimate of the activation energy; so the value of 1.32 eV observed by Tatibouet *et al.* (1987) is employed. The results further indicate that the pre-exponential in the relaxation time expression should be in the range  $2.7 \times 10^{-27} - 8 \times 10^{-28} \text{ s}$ , which corresponds to a range in the peak location of approximately  $5^\circ\text{C}$ . The model employs the lower value, which is commensurate with the order of magnitude value of  $10^{-28} \text{ s}$  reported by Tatibouet *et al.* (1987).

The  $18^\circ\text{C}$  width at half-height for the grain-boundary peak corresponds to  $\alpha^{gb} \approx 0.6$  in eqn. (9). This value reproduces the grain-boundary peak observations in saline ice reasonably well and is employed in the analysis. As in the case of the dislocation relaxation,  $\alpha^{gb}$  depends on the distribution of relaxation times associated with the grain-boundary relaxation and its value could change for significantly different microstructures. Although the peak characteristics may be influenced by the presence of brine- and gas-filled inclusions, a comparison of the grain-boundary internal-friction peaks observed in freshwater and saline ice (Cole 1994) showed them to be very similar to magnitude and width. The model uses  $\delta D_2^{gb} = 3 \times 10^{-11} \text{ Pa}^{-1}$ , which corresponds to  $D_2^{gb} \text{ max} = 9 \times 10^{-12} \text{ Pa}^{-1}$  and is appropriate for grain sizes in the range 3–10 mm. Adding the dislocation contribution of  $D_2^d = 2.3 \times 10^{-12} \text{ Pa}^{-1}$  produces a peak value

Fig. 6



Model predictions for compliance against temperature for 1 Hz illustrating the grain-boundary peak and dislocation contribution.

of the observed height, as seen in fig. 6. The transient in the grain-boundary relaxation has been calculated in the manner discussed in the preceding section. Frequencies and temperatures of practical interest are typically well below the relaxation peak, with the result that the strain associated with this relaxation is primarily in phase with the applied stress, contributing to the modulus defect.

§ 6. COMPARISON WITH EXPERIMENTAL OBSERVATIONS

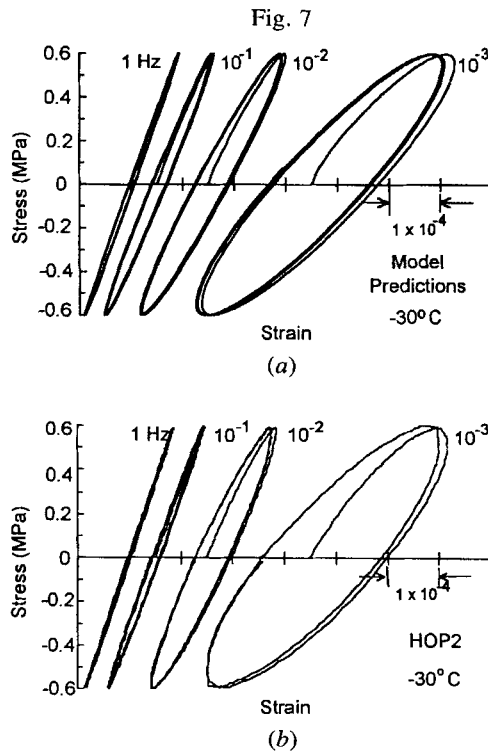
In the absence of deformation that would effectively lock the grain boundaries, both the grain boundary and dislocation relaxations are expected to operate simultaneously so  $D_1 = D_1^d + D_1^{gb}$  and  $D_2 = D_2^d + D_2^{gb}$  (see curves labelled Total in fig. 3), where

$$\begin{aligned}
 D_1^d(\omega) &= D_u^d + \delta D^d \left( 1 - \frac{2}{\pi} \tan^{-1} [\exp(\alpha^d s_1^d)] \right), \\
 D_2^d(\omega) &= \alpha^d \delta D^d \frac{1}{\exp(\alpha^d s_1^d) + \exp(-\alpha^d s_1^d)}, \\
 D_1^{gb}(\omega) &= D_u^{gb} + \delta D^{gb} \left( 1 - \frac{2}{\pi} \tan^{-1} [\exp(\alpha^{gb} s_1^{gb})] \right), \\
 D_2^{gb}(\omega) &= \alpha^{gb} \delta D^{gb} \frac{1}{\exp(\alpha^{gb} s_1^{gb}) + \exp(-\alpha^{gb} s_1^{gb})}.
 \end{aligned}
 \tag{16}$$

The superscripts d and gb indicate quantities pertaining to the dislocation and grain boundary relaxations respectively;  $s_1^d = \ln(\tau^d \omega)$  and  $s_1^{gb} = \ln(\tau^{gb} \omega)$ . The transients in both relaxations are governed by eqn. (15) with the appropriate values of the peak-broadening term and relaxation time.

Figure 7 compares hysteresis loops obtained from the model with experimental results and fig. 8 illustrates the temperature and frequency dependences of the modulus for the first and second loading cycles. Plots of experimental data appear to the right in these figures, and the predicted first cycle moduli were calculated for approximately the same total strain level ( $\epsilon$  of the order of  $10^{-5}$ ) as the values calculated from the experimental data.

Figure 9 compares the predicted hysteresis loop widths with results for a single specimen from Cole and Durell (1995). The grain-boundary peak is primarily evident in the 1 Hz results. It becomes only vaguely evident at the lower frequencies as it shifts



Comparison of model predictions and experimental observations for  $T = -30^\circ\text{C}$ ,  $\pm 0.6\text{ MPa}$  and the four test frequencies. (a) Model predictions with a dislocation density of  $1.8 \times 10^9\text{ m}^{-2}$ ,  $\alpha^d = 0.54$  and  $K = 0.07$ . Other than the input frequency, there were no parameter changes in the model for the various loops. (b) Stress-strain loops from specimen HOP2 (Cole and Durell 1995). The loops have been shifted by arbitrary amounts along the strain axis for clarity.

to lower temperatures and as the magnitude of the dislocation contribution increases significantly. The predictions are based on a single set of values for all the model parameters. A value of  $9.0\text{ GPa}$  has been used for the unrelaxed modulus in all cases, which is representative of the results presented by Cole and Durell (1995).

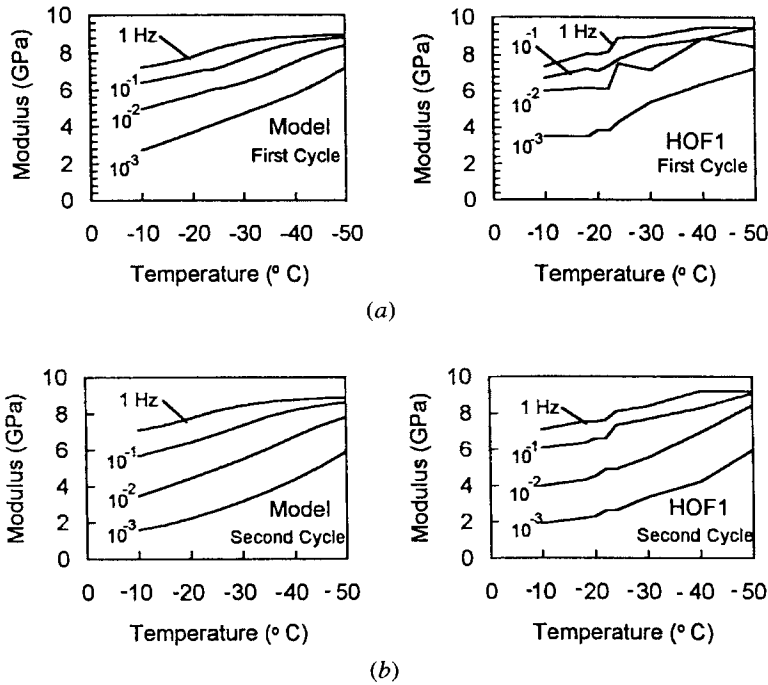
### § 7. DISCUSSION

The model yields very reasonable predictions of the transient and steady-state cyclic loading response of laboratory-prepared saline ice over the stated range of loading and environmental conditions. Although simplified in certain respects, the model captures the main features of the response and provides a physically based framework for further development.

The activation energies for the two mechanisms adequately describe the observed temperature dependence for  $T \leq -10^\circ\text{C}$ . Apart from the activation energies and perhaps the central relaxation time for the grain-boundary process, the other model parameters ( $\delta D^d$ ,  $\alpha^i$ ,  $K$ ,  $\Delta$  and  $\Omega$ ) are functions of the particular microstructure and defect structure.

The quantities  $\delta D^d$  and  $\delta D^{gb}$  determine the maximum anelastic strain associated with each mechanism. As indicated in eqn. (14),  $\delta D^d$  increases with increasing mobile dislocation density and decreases with increasing opposing stress  $K$ . Calculations

Fig. 8



Model predictions of the initial modulus as a function of temperature for four loading frequencies for the initial tensile loading for (a) the first cycle and (b) the second cycle. The figures on the left are calculated from the model and the adjacent figures on the right are experimental results from specimen HOF1 (Cole and Durell 1995).

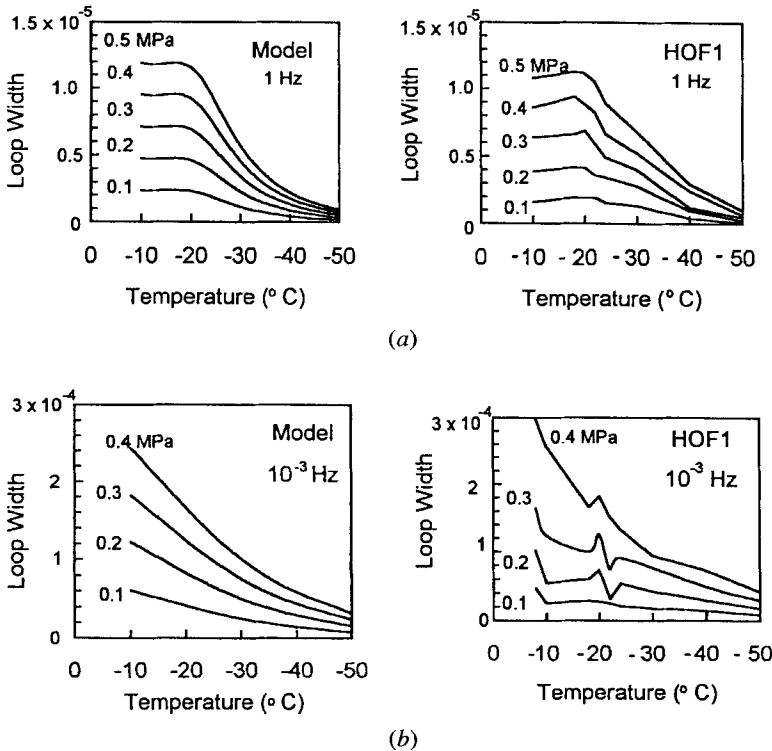
indicate that the variations in compliance associated with the range in specimen porosity stated by Cole and Durell (1995) correspond to a fifteenfold increase in the mobile dislocation density.

Although held constant at a representative value for larger grain sizes,  $\delta D^{gb}$  clearly depends on the details of the microstructure. The associated anelastic strain is of the order of the elastic strain, in keeping with observations of grain-boundary sliding in other materials (Gibeling and Nix 1981). As noted earlier, the strength and relaxation times of grain-boundary sliding in ice appear to be very similar to those in some metals. The ease with which a wide range of microstructures can be produced and optically examined in ice recommends this material for use in detailed studies of grain-boundary processes.

The parameters  $\alpha^d$  and  $\alpha^{gb}$  (which control the peak widths for each relaxation process) are functions of the relaxation time distributions for each mechanism and can be determined from the cyclic loading response over a range of frequencies at a fixed temperature. Although they are expected to depend on microstructure, they appear to vary little for the laboratory-prepared ice examined thus far.

The value of  $K = 0.07$  Pa, estimated from the experimental results, is lower than the value of about 0.5 Pa calculated by Joncich (1976) for deformed ice single crystals. It is lower still than the value of 3.2 Pa calculated from the expression  $3\mu b^2 N$  given by Weertman (1955) for metal single crystals. The reasons for the disagreement are unclear at present. It is noted, however, that, since the relaxation time is  $\tau^d = B/K$ , significantly

Fig. 9



Comparison of model predictions (on the left) and typical experimental results (on the right) for loop width against temperature for peak cyclic stress levels as indicated, and loading frequencies of (a) 1 Hz and (b)  $10^{-3}$  Hz. Experimental results are from specimen HOF1 from the work of Cole and Durell (1995).

greater values of  $K$  would lead to implausibly short relaxation times for the dislocation peak.

The independent assessment of the dislocation density  $\Delta$ , a key quantity in the model, presents a problem since typical values for saline ice are much too high to be reliably determined from X-ray topographs. Although an eventual goal in this regard is to estimate  $\Delta$  from known growth conditions, for the near term it appears necessary to estimate an effective value from laboratory compliance measurements.

An important feature of the model is the incorporation of the effects of a relaxation time distribution, which explains both the frequency dependence of the anelastic straining and the transient behaviour observed from the start of loading. As noted by Cole and Durell (1995), the hysteresis loops are generally not centred on the point ( $\epsilon = 0, \sigma = 0$ ) during nominal steady-state cycling but tend to have an offset in the direction of the initial loading direction. The model reproduces this behaviour because the relaxation time distribution provides for relaxation times longer than the duration of the experiments. It is noted that the present treatment assumes that the relaxation time distribution is symmetrical about its peak, but this need not be the case.

Improvements to the model will incorporate the relatively minor temperature dependence of the elastic modulus (Hobbs 1974) and the dependence of the modulus on the net porosity of the specimen (Cox and Weeks 1983). Such effects are expected

to become very strong for  $T > -10^{\circ}\text{C}$ , which is above the range of applicability of the present formulation. These effects will be incorporated as the model is extended to higher temperatures.

Although the two mechanisms are treated independently, grain boundaries can influence the magnitude of the dislocation relaxation when pre-strain or annealing effects are considered (Narutani and Takamura 1991, Llanes, Rollet, Laird and Bassani 1993). A grain size effect might occur in the dislocation mechanism since the population of dislocation sources such as grain-boundary ledges and triple points scale with the grain-boundary area.

Grain-boundary sliding promotes stress concentrations at ledges and triple points and thereby enhances crack nucleation (Evans 1980). In the flow with cracking regime (from approximately  $10^{-6}$  to  $10^{-3}\text{ s}^{-1}$  at  $-10^{\circ}\text{C}$ ), ice exhibits a shift from mixed intergranular and intragranular cracking with appreciable dislocation activity at the lower rates to grain-boundary cracking accompanied by very little dislocation activity at high strain rates (Gold 1972, Cole 1986). This trend coincides with the shift from dislocation- to grain-boundary-dominated anelasticity predicted by the model (see fig. 3) at about 1 Hz at  $-10^{\circ}\text{C}$ .

#### § 8. CONCLUSIONS

The anelastic strain of saline ice for constant microstructural conditions is well represented by a model based on a dislocation relaxation and a grain-boundary relaxation. In saline ice, which has a characteristically high dislocation density, the dislocation relaxation generally dominates the cyclic loading response. The activation energy for the dislocation process, which comes from the dislocation drag term, was assessed by cyclic loading experiments and found to be effectively the same for both fresh-water and saline ice. Laboratory-prepared saline ice exhibits a distinct grain-boundary relaxation peak as found in fresh-water ice, despite the presence of gas- and brine-filled inclusions along grain boundaries. The relaxation peaks for both processes were broadened by the effects of a distribution in relaxation times. A peak-broadening term in the frequency function adequately modelled the frequency response, simplified calculations and provided a convenient means for determining the transient response.

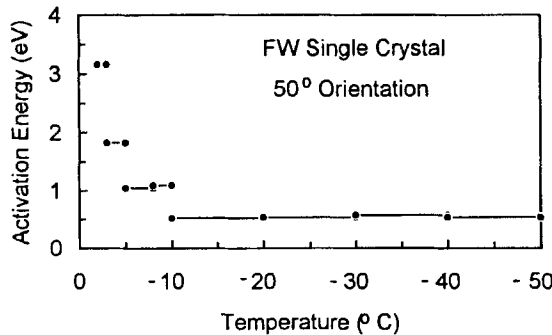
A direct comparison with experimental results demonstrated that the model adequately reflects the main features of the transient and steady state cyclic loading behaviour.

The model provides a framework for continued development and current efforts focus on the incorporation of explicit microstructural effects on the parameters, developing a temperature- and microstructure-dependent expression for the elastic modulus, and extending its range of applicability to higher temperatures and lower frequencies.

#### ACKNOWLEDGMENTS

The author gratefully acknowledges the support of the Office of Naval Research and the US Army Cold Regions Research and Engineering Laboratory and expresses his appreciation to Professor J. Weertman of Northwestern University for enlightening discussions regarding dislocation processes, to Professor R. Schapery of the University of Texas, Austin, for many helpful comments and discussions, and to Professor H. Frost and I. Baker of Dartmouth College for helpful discussions.

Fig. A 1



Apparent activation energy from a frequency shift analysis of single-crystal data. The average value for temperatures below  $-10^{\circ}\text{C}$  is  $0.54\text{ eV}$ .

#### APPENDIX

An estimate of the temperature dependence of the oscillatory motion of basal dislocations was determined from experiments on a single crystal of fresh-water ice oriented for easy glide, employing the same experimental technique as used in the saline-ice experiments. The single-crystal experiments will be described in detail in a forthcoming paper. The activation energy was determined by the frequency shift analysis described in the text.

The dislocation velocity in ice has been shown to be a linear function of stress at relatively low stresses and a simple exponential function of temperature (see the review by Whitworth (1978)):

$$v_d = A\sigma \exp\left(-\frac{Q}{kT}\right), \quad (\text{A } 1)$$

where  $v_d$  is the velocity of basal dislocations,  $A$  is a proportionality constant,  $\sigma$  is the shear stress on the basal plane and the other terms have their usual meanings. For temperatures below approximately  $-10^{\circ}\text{C}$ , for stresses in the range of the present experiments, and assuming linearity, Mai (1976) reports an activation energy of  $0.55 \pm 0.05\text{ eV}$  for basal dislocations observed with X-ray topography. As pointed out by Whitworth (1978), the activation energy determined from those data can vary, depending on how one accounts for the nonlinearity evident at higher temperatures. However, examination of the results indicates that the linear assumption is reasonable for temperatures below approximately  $-10^{\circ}\text{C}$ .

The analysis of the experimental results on an oriented single crystal by the present author included temperatures of  $-2$ ,  $-3$ ,  $-5$ ,  $-10$ ,  $-20$ ,  $-30$ ,  $-40$  and  $-50^{\circ}\text{C}$ , stress levels of  $\pm 0.4$ ,  $\pm 0.6$  and  $\pm 0.8\text{ MPa}$ , and frequencies of  $1$ ,  $10^{-1}$ ,  $10^{-2}$  and  $10^{-3}\text{ Hz}$ . Figure A 1 shows the calculated values of the apparent activation energy. The values are plotted as bars extending over the temperature interval used for the calculation. Estimates of the creep effects have been removed from the results for the values obtained at  $10^{-3}\text{ Hz}$ . The data exhibit a sharp rise for temperatures above  $-10^{\circ}\text{C}$  and sustain a relatively constant value, averaging  $0.54\text{ eV}$ , between  $-10$  and  $-50^{\circ}\text{C}$ . This value closely agrees with the activation energy observed by Mai (1976) as noted above.

The drag term and velocity are related to the applied stress by the following relationship:

$$Bv_d = b\sigma. \quad (\text{A } 2)$$

Substituting for the velocity from eqn. (A 1) yields

$$B(T) = \frac{b}{A} \exp\left(\frac{Q}{kT}\right). \quad (\text{A } 3)$$

Thus the term  $B_0$  in eqn. (5) in the text has the value  $b/A$ . The results of Fukuda and Higashi (1973) allow an estimate of  $A$ . For observations at  $-18^\circ\text{C}$ , they report a stress dependence in the form

$$v_d = c\sigma, \quad (\text{A } 4)$$

where the constant  $c$  absorbs the exponential term and varies with the geometry of the dislocation line. Using an average value of  $c = 5.1 \times 10^{-12} \text{ m}^3 \text{ N}^{-1} \text{ s}^{-1}$ , and an activation energy of 0.55 eV, yields  $A = 0.375$ . This in turn produces a value of  $B_0 = 1.205 \times 10^{-9} \text{ Pa s}$ . The temperature-dependent drag term is thus given by

$$B(T) = 1.205 \times 10^{-9} \exp\left(\frac{0.55}{kT}\right), \quad (\text{A } 5)$$

where  $B(T)$  has unit of partial seconds.

#### REFERENCES

- COLE, D. M., 1986, US Army Cold Regions Research and Engineering Laboratory, Hanover, New Hampshire, Report No. 86-5; 1991, *Proceedings of the Sixth International Specialty Conference on Cold Regions Engineering*, Lebanon, NH, 26-28 February 1991, edited by D. Sodhi (New York: American Society of Civil Engineers), pp. 504-518; 1992, *Hydrostatic Pressure Effects on the Internal Friction and Creep of Ice*, Ph.D. Thesis, Northwestern University, Evanston, Illinois; 1993, *Ice Mechanics-1993, Proceedings of the First Joint Mechanics Meeting of the American Society of Mechanical Engineers, American Society of Civil Engineers and the Society of Engineering Science*, Charlottesville, Virginia, 6-9 June 1993, Applied Mechanics Division (New York: American Society of Mechanical Engineers), Vol. 163, pp. 261-272; 1994, *Proceedings of the International Association of Hydraulic Research Twelfth International Ice Symposium*, Vol. III, Trondheim, 23-26 August 1994 (Trondheim: The Norwegian Institute of Technology), pp.1051-1059.
- COLE, D. M., and DURELL, G., 1995, *Phil. Mag. A*, **72**, 209.
- COX, G. F. N., and WEEKS, W. F., 1983, *J. Glaciol.*, **29**, 306.
- DUVAL, P., 1978, *J. Glaciol.*, **21**, 621.
- EVANS, A. G., 1980, *Acta metal. mater.*, **28**, 1155.
- FERRY, J. D., 1981, *Viscoelastic Properties of Polymers* (New York: Wiley).
- FUKUDA, A., and HIGASHI, A., 1973, *Crys. Lattice Defects*, **4**, 203.
- FUKUDA, A., HONDOH, T., and HIGASHI, A., 1987, *J. Phys., Paris*, **48**, C1-163.
- GIBELING, J. C., and NIX, W. D., 1981, *Acta metall.*, **29**, 1769.
- GOLD, L. W., 1958, *Can. J. Phys.*, **36**, 1265; 1972, *Phil. Mag.*, **26**, 311; 1994, *Ann. Glaciol.*, **19**, 13.
- HIKI, Y., and TAMURA, J., 1983, *J. phys. Chem.*, **87**, 4054.
- HOBBS, P. V., 1974, *Ice Physics* (Oxford: Clarendon), p. 837.
- JONCICH, D. M., 1976, Ph.D. Thesis, University of Illinois at Urbana-Champaign, 97 pp.
- KÊ, T. S., CUI, P., YAN, S. C., and HUANG, Q., 1984, *Phys. Stat. sol. (a)*, **86**, 593.
- KHUSNATDINOV, N. K., and PETRENKO, V. F., 1994, *Phys. Rev. Lett.*, **72**, 3363.
- KRESSEL, H., and BROWN, N., 1967, *Dislocation Dynamics*, edited by A. R. Rosenfield, G. T. Hahn, A. L. Bement and R. I. Jaffee (New York: McGraw-Hill), pp. 337-356.

- KUROIWA, D., 1965, US Army Cold Regions Research and Engineering Laboratory Research Report No. 131.
- LAKKI, A., SCHALLER, R., NAUER, M., and CARRY, C., 1993, *Acta metall. mater.*, **41**, 2845.
- LENZ, D., and LÜCKE, K., 1975, *Proceedings of the Fifth International Conference on Internal Friction and Attenuation in Solids*, Aachen, 1975, Vol. 2 (Berlin: Springer), pp. 48–108.
- LIU, F., BAKER, I., YAO, G., and DUDLEY, M., 1992, *Mater. Sci.*, **27**, 2719.
- LLANES, L., ROLLETT, A. D., LAIRD, C., and BASSANI, J. L., 1993, *Acta metall. mater.*, **41**, 2667.
- MAI, C., 1976, *C. hebd. Séanc. Acad. Sci., Paris, Sér. B*, **282**, 515.
- MASON, W. P., 1967, *Dislocation Dynamics*, edited by A. R. Rosenfield, G. T., Hahn, A. L., Bement, and R. I. Jaffee (New York: McGraw-Hill), pp. 487–505.
- NAKAMURA, T., and ABE, O., 1979, *J. Fac. Sci., Hokkaido Univ. Ser. VII (Geophys.)*, **6**, 165.
- NARUTANI, T., and TAKAMURA, J., 1991, *Acta metall. mater.*, **39**, 2037.
- NOWICK, A. S., and BERRY, B. S., 1972, *Anelastic Relaxation in Crystalline Solids* (New York: Academic Press), 677 pp.
- ONSAGER, L., and RUNNELS, L. K., 1969, *J. chem. Phys.*, **50**, 1089.
- SHEARWOOD, C., and WHITWORTH, R. W., 1991, *Phil. Mag. A*, **64**, 289.
- SHIGENAKA, N., MONZEN, R., and MORI, T., 1983, *Acta metall. mater.*, **31**, 2087.
- SINHA, N. K., 1978, *Exp. Mech.*, 464; 1979, *Proceedings of the Workshop on the Bearing Capacity of Ice Covers*, Winnipeg, Manitoba, 16–17 October 1978, pp. 65–77; 1990, *Proceedings of the Fourth International Conference on the Creep and Fracture of Engineering Materials and Structures*, Swansea 1990, edited by B. Wilshire and R. W. Evans.
- TATIBOUET, J., PEREZ, J., and VASSOILLE, R., 1987, *J. Phys., Paris, Suppl. 3*, **48**, C1–197.
- VASSOILLE, R., MAI, C., and PEREZ, J., 1978, *J. Glaciol.*, **21**, 375.
- WEERTMAN, J., 1955, *J. appl. Phys.*, **26**, 202; 1983, *A. Rev. Earth planet. Sci.*, **11**, 215.
- WHITWORTH, R. W., 1978, *J. Glaciol.*, **21**, 341.
- WOIRGARD, J., RIVIERE, A., and DE FOUQUET, J., 1981, *J. Phys., Paris, Suppl. 10*, **42**, C5–407.